Trident Production Cross Section and Quantum Electrodynamics at Small Distances*

MAO-CHAO CHEN†
Department of Physics and Institute of Theoretical Physics, Stanford University, Stanford, California
(Received April 2, 1962)

The cross section has been calculated for the coincidence experiment of electron–positron pair production from electron–proton collisions as a test of quantum electrodynamics at small distances. The electrons and positrons are considered highly relativistic and the protons are considered as Coulomb field sources; otherwise the calculations are exact to the fourth order of the matrix element. Distances probed are about 0.5 F.

INTRODUCTION

THE validity of quantum electrodynamics (QED) at small distances and related experiments have been discussed in earlier papers.[1–3] In reference 3 the trident experiment, i.e., electron-positron pair production from high-energy electron–proton collision, has been proposed. To the fourth order of the matrix element there are eight Feynman diagrams as shown in Fig. 1. As discussed in reference 1, if the photon propagator $1/q^2$ is modified by $(1+d^2q^2)/q^2$ at high q^2, where q is the four-momentum carried by the photon line, then d, being of dimension length, is a measure of the validity of QED at small distances. This modification has no *a priori* justification or fundamental significance. It is used simply to provide a convenient way of characterizing deviations from the present theory when interactions with virtual photons are being studied. Therefore, to test the upper limit of d, very virtual photons with large q^2 are to be considered.

In the present experiment the electron and positron are to be detected by coincidence. For simplicity they are observed at equal energies, lying in the same plane with the incident electron, and at the same scattering angle and lying side by side with respect to the incident beam. In Fig. 1 the electron with four-momentum p_1 and positron with four-momentum p_+ are to be observed, while the electron with four-momentum p_2 is not observed.

In Fig. 1(a) the square of four-momentum transfer $(p-p_1)^2$, p being the four-vector of the incident electron, of the photon line connecting the incident electron line is constant and fixed by the experiment, i.e., by the choice of the scattering angle θ in the coincidence experiment. The measured cross section is proportional to the square of this photon propagator. This diagram is a good diagram from the point of view of investigating the photon propagator, because any modification of the photon propagator at high momentum transfer is reflected in the observed cross section. Diagrams (b), (g), and (h) in Fig. 1 all possess this property and are all good diagrams. On the other hand, in diagram (c) the momentum transfer $(p-p_2)^2$ depends on the momentum p_2 of the unobserved electron which can be of any magnitude and along any direction. When $\mathbf{p}_2$ is parallel to $\mathbf{p}$, $(p-p_2)^2$ becomes very small, and the propagator and cross section become very large. The main contribution to this diagram comes from the photon which is nearly real. This diagram is bad because any

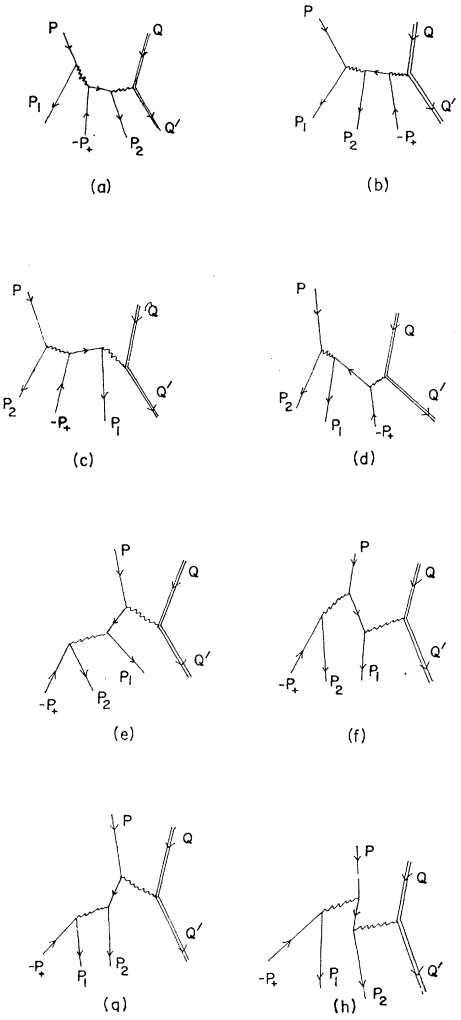

FIG. 1. Fourth-order production diagrams.

* Supported in part by the U. S. Air Force through the Air Force Office of Scientific Research.
† Present address: Laboratory for Nuclear Science and Physics Dept., Massachusetts Institute of Technology, Cambridge, Massachusetts.
[1] S. D. Drell, Ann. Phys. (New York) **4**, 75 (1958).
[2] J. D. Bjorken, S. D. Drell, and S. Frautschi, Phys. Rev. **112**, 1409 (1958).
[3] J. D. Bjorken and S. D. Drell, Phys. Rev. **114**, 1368 (1959).

modification at high momentum transfer would have little effect on the cross section. The remaining three diagrams (d), (e), and (f) all have this property and are bad diagrams. Despite the large cross section of bad diagrams, the good diagrams can still dominate if we choose the scattering angle θ around the forward direction. We must choose $\theta \gg m/E$ in order to probe QED at small distances but $\theta < 1$ radian to obtain a finite counting rate. As shown in reference 3, the good diagrams are important in this region, while the bad diagrams contain only logarithmic terms to order E/m. Some of the good diagrams in reference 3 become bad diagrams in our case, and vice versa. This is because two final electrons are observed in reference 3, while a positron and an electron are observed in our case. Therefore, Figs. 1(c) and 1(d) are good ones in reference 3 but bad ones in our case, if the electron we are not observing has momentum p_2. Though some good and bad diagrams are interchanged, the theorems proved in Appendix I of reference 3 can still apply, i.e., good diagrams are more important than the bad diagrams.

The calculated cross section is then compared with experiments allowing uncertainties. Disagreements between these results would indicate a breakdown of QED of virtual photon amplitudes at high-momentum transfer or at small distances, if there is no deviation originating from the electron lines. The electron propagator can be tested by a separate experiment, the electron–positron pair production from photon-proton collision.[1,2] Alternately, we can observe the ratio of cross sections between the two experiments. In this case, any high-momentum transfer modification of electron line would have little effect on the ratio, as has been discussed in reference 3.

Some limiting cases of the trident cross section have been discussed in reference 3. In the present treatment, the cross section is calculated more exactly and the final formulas are valid for a broad range of realistic experimental parameters. All electrons and positrons are considered extremely relativistic; otherwise, their energies and directions are arbitrary. The proton is treated as a Coulomb field source. All square and interference terms are included. In our symmetrical arrangement four terms cancel one another, and the remaining 32 terms can be integrated in terms of elementary functions. However, the results are very complicated, and instead we evaluate only several numerical values.

CALCULATION

The calculation is straightforward. The S-matrix element is written down by the Feynman rule. Following the standard procedure,[4] with the approximation and experimental situation stated above, we find the differential cross section $d\sigma$ of observing an electron within the energy range dE_1, the solid angle $d\Omega_1$, and simultaneously a positron within the energy range dE_+, the solid angle $d\Omega_+$:

$$d\sigma=\frac{\alpha^4}{32\pi^4}\frac{E_2E_1E_+}{E}\sum_{(i,j=a,b,c,d,e,f,g,h)}I_{ij}dE_1dE_+d\Omega_1d\Omega_+,$$

where

$$I_{ij}=I_{ji}\equiv\int_0^\pi\int_0^{2\pi}\frac{N_{ij}}{D_iD_j}\sin\theta_2d\theta_2d\varphi_2,$$

$$D_a=-\alpha(\alpha+\beta-\gamma)f_1, \quad D_b=-\alpha f_1g,$$

$$D_c=-f_1f_2g_2, \quad D_d=-f_1f_2g,$$

$$D_e=-f_1f_3g_3, \quad D_f=f_1g_2g_3,$$

$$D_g=-\gamma f_1f_3, \quad D_h=\gamma(\alpha+\beta-\gamma)f_1,$$

and

$$\alpha\equiv p\cdot p_1, \quad \beta\equiv p\cdot p_+, \quad \gamma=p_1\cdot p_+.$$

$$f_1=-\tfrac{1}{2}(p-p_1-p_2-p_+)^2, \quad f_2=-\tfrac{1}{2}(p-p_2)^2,$$

$$f_3=\tfrac{1}{2}[(p_1+p_2+p_+)^2-m^2], \quad g_1=\tfrac{1}{2}[m^2-(p_1+p_2-p)^2],$$

$$g_2=\tfrac{1}{2}[m^2-(p-p_2-p_+)^2], \quad g_3=\tfrac{1}{2}(p_2+p_+)^2.$$

α, β, and γ are constant (independent of θ_2, φ_2).[5] The functions f_i depend on θ_2 only, g_i depend on θ_2 and φ_2. The numerators N_{ij} are complicated trace functions due to the interference between various diagrams. For instance, N_{ab} is due to the interference between diagrams a and b, N_{aa} is the square term of diagram a, etc. A typical term which contributes most to the cross section is

$$N_{ee}=\tfrac{1}{64}\,\mathrm{Tr}(p_1\gamma^\mu p_e\gamma^0p\gamma^0p_e\gamma^\nu)\,\mathrm{Tr}(p_2\gamma_\mu p_+\gamma_\nu),$$
$$p_e\equiv p_1+p_2+p_+.$$

These N_{ij} have some exchange properties without reference to the symmetry of p_1 and p_+. For instance, under an exchange of parameters

$$p\leftrightarrow -p_1, \quad E\leftrightarrow -E_1,$$

we find N_{ee} is changed into N_{ff}. Thus, we find that N_{ij} can be divided into five groups such that in each group only the trace of one N_{ij} needs to be evaluated explicitly, the rest can be obtained by their exchange properties. These five groups are (1) N_{ii}, $i=a, b, \cdots h$, (2) N_{af}, N_{be}, N_{bf}, N_{ae}, N_{ch}, N_{dh}, N_{cg}, N_{dg}, (3) N_{bc}, N_{ce}, N_{df}, N_{fg}, N_{ag}, N_{bh}, N_{ad}, N_{eh}, (4) N_{ef}, N_{cd}, N_{gh}, N_{ab}, (5) N_{ac}, N_{ah}, N_{bd}, N_{bg}, N_{cf}, N_{de}, N_{eg}, N_{fh}. The term N_{ee} mentioned above after the trace has been evaluated ex-

[4] S. S. Schweber, H. A. Bethe, and F. de Hoffman, *Mesons and Fields* (Row, Peterson and Company, Evanston, Illinois, 1955), Vol. I.

[5] We use the metric $A\cdot B=A_0B_0-\mathbf{A}\cdot\mathbf{B}$.

plicitly is

$$N_{ee}=\tfrac{1}{64}\{2E^2[(p_2\cdot p_1)(p_2\cdot p_+)+2\gamma p_2\cdot p_1+\gamma p_2\cdot p_+]$$
$$-2EE_+p_2\cdot p_1(p_2\cdot p_++p_2\cdot p_1+\gamma)$$
$$-2EE_2\gamma(p_2\cdot p_++p_2\cdot p_1+\gamma)$$
$$-(p_2\cdot p_1)(p_2\cdot p)(p_2\cdot p_+)-\gamma(p_2\cdot p)(p_2\cdot p_1)$$
$$-\alpha(p_2\cdot p_1)(p_2\cdot p_+)+\beta(p_2\cdot p_1)^2-\gamma(2\alpha+\beta)p_2\cdot p_1$$
$$-\gamma(\alpha+\beta)p_2\cdot p_++\gamma^2p_2\cdot p\}.$$

Five N_{ij} have been evaluated.[6]

The angular integrals I_{cg} and I_{ch} are found equal to $-I_{dg}$ by rotating 180° about the z axis for our case of symmetrical choice of p_1 and p_+. Therefore they cancel with each other. All integrals I_{ij} can be integrated explicitly in terms of elementary functions. This is done by decomposing the integrand N_{ij}/D_iD_j into the sum of partial fractions whose denominators are of the form $(f_i)^n$ or $(g_i)^n$, n integer. Then it is easy to see that these partial fractions can be integrated. However, the result would be very complicated. Instead, the angular integrals are carried out by the Burroughs 220 computer for several numerical cases.

On the other hand, we obtain an approximate expression in the limiting case $E_2/E(1-\lambda)\ll 1$,

$$d\sigma=dE_1dE_+d\Omega_1d\Omega_+\frac{\alpha^4}{\pi^3E^4(1-\lambda)^3}$$
$$\times\left\{\frac{15+21\lambda+13\lambda^2+3\lambda^3}{4(1+\lambda)(1-\lambda)^3}\left(\frac{E_2}{E}\right)^2+\frac{3+2\lambda}{8}\ln\frac{2E_2}{m}\right\},$$

$\lambda\equiv\cos\theta$.

The interference terms between good and bad diagrams are small and neglected in the above approximate expression.

CONCLUSION AND DISCUSSION

The numerical integration from the Burroughs 220 computer gives the following result for $\theta=22.5°$:

E (MeV)	E_2 (MeV)	E_1 ($=E_+$) (MeV)	$\frac{d\sigma}{dE_1dE_+d\Omega_1d\Omega_+}\left(\frac{\text{cm}}{\text{MeV-sr}}\right)^2$
500	100	200	5.6×10^{-37}
500	50	225	6×10^{-37}
550	150	200	3.6×10^{-37}
550	100	225	3×10^{-37}

The integrals I_{ee}, I_{ef}, I_{ff} have very strong peaks near the positron direction and the computer results converge very slowly. Their sum, $I_{ee}+2I_{ef}+I_{ff}$, is the difference among large and nearly equal numbers. Therefore approximate analytical integrations are carried out for this sum. It turns out that the highest order in E/m appearing in the sum is $\ln(E/m)$, as has been proved generally in the Appendix of reference 3.

If the photon propagator is modified by the factor $[1+d^2(p-p_1)^2]$, the cross sections of the good diagrams will be modified by the square of this factor, that of the bad diagrams will not be changed, and the interference terms between good and bad diagrams will be modified by the factor alone. If $d\sigma'$ denotes the experimental cross section and r the ratio of the cross sections of good diagrams plus half the interference term between good and bad diagrams to the total experimental cross section, then d^2 is given by

$$d^2=\frac{d\sigma-d\sigma'}{d\sigma}\frac{1}{r}\frac{1}{[-2(p-p_1)^2]}.$$

The ratio r as evaluated in numerical integration, and the distance d probed correspond to two given experimental discrepancies shown as follows:

E (MeV)	E_2 (MeV)	r	d (10^{-13} cm) for $(d\sigma-d\sigma')/d\sigma'=10\%$, $=15\%$	
500	100	0.8	0.4	0.49
500	50	0.72	0.39	0.48
550	150	0.83	0.37	0.45
550	100	0.79	0.37	0.45

In our calculation of the cross section, several effects have been neglected: finite proton mass, proton magnetic moment and form factor, and the higher order radiative correction. Qualitatively, the first three are of the order 1%, −2%, and −4%, respectively. The radiative correction, estimated on the basis of the Schwinger correction $-(4\alpha/\pi)\ln(E/m)\ln(E/E_2)$, is about −9%. When compared with experimental result, these effects should be taken into account.

Criegel[7] has measured the cross section for all positron angles and all electron energy and angles for 30-MeV incident electron. This energy is too small to give information at small distances. However, it can be used to check that experiments and calculations do agree in the low-energy range, with proper radiative corrections.

ACKNOWLEDGMENTS

The author is indebted to Professor S. D. Drell for suggesting this problem and his constant guidance throughout the work. He also wishes to thank Dr. Y.-S. Tsai for many helpful discussions.

[6] For the other terms see M.-c. Chen, Ph.D. dissertation, Stanford University, 1962 (unpublished).

[7] L. Criegel, Z. Physik **158**, 433 (1960). We thank Dr. Creige for bringing this to our attention.